# Niobium coated Ti-Al alloy: improvement of tribological behaviour, oxidation resistance and flame retardancy

Xiangfei Wei [a, *], Pingze Zhang [a], Dongbo Wei [a], Hongyuan Zhao [b], Tomasz Liskiewicz [b]

[a] College of Materials Science and Technology, Nanjing University of Aeronautics and Astronautics, Nanjing, 211106, China.

[b] School of Mechanical Engineering, University of Leeds, Leeds, LS2 9JT, UK.

*Corresponding author: wxf1018@nuaa.edu.cn

**Abstract:** Double glow plasma (DGP) coatings were recommend for metallic components to mitigate the damage induced by complex working conditions. In this paper, A Ti-Al alloy was coated with niobium (Nb) via a DGP process to enhance its anti-oxidation properties, wear resistance and flame retardancy. The results showed that the Nb-coated Ti-Al alloy mainly comprised Nb, AlNb2, AlMoTi2 and β-Ti phases. Room temperature sliding-friction tests indicated that the Nb-coated Ti-Al alloy exhibited a stable friction coefficient of an average value of 0.25, whilst the same value for via the uncoated Ti-Al alloy was around 0.45. High-temperature oxidation tests revealed compact oxide grains without cracks after the 100 h test, indicating good oxidation resistance. An ablation test showed that the Nb-coated Ti-Al alloy exhibited excellent flame retardancy, with the ablation time of the Nb-coated Ti-Al alloy at 1.62 times that of the uncoated Ti-Al base alloy. The alloy's tribological behaviour, oxidation resistance and flame retardancy mechanisms are discussed in detail in this paper.

**Keywords:** Double glow plasma technique; Nb-coated Ti-Al; wear resistance; high temperature oxidation resistance; flame retardancy.

## 1. Introduction

Titanium and titanium alloys are excellent candidates for aerospace applications, due to their high strength-to-weight ratio and excellent resistance to corrosion (Peters et al., 2003); Wagner, and Wollmann, 2013). However, for rotating components in high-performance engines, titanium's low transition temperature often presents a challenge. At elevated temperatures and in a high-pressure air environment, this can lead to a very rapid oxidation of the titanium. The oxidation process, which is exothermic, can become self-propagating and cause the burning of the titanium (Leyens, and Peters, 2003); Zhao et al., 2000).

There are typically two approaches to solving this challenge. One is adding alloying elements during smelting, and the other is applying a surface modification. The Ti alloys with Nb added as an alloying element have been shown to possess flame-retardant properties and superior corrosion resistance (Godley et al., 2006); Wang et al., 2004). At the same time, the surface modification techniques have few negative effects on the mechanical performance of the substrates, such as physical vapour deposition (Nolan et al., 2006)., plasma nitriding (El-Hossary et al., 2015). and ion plating (Rautray et al., 2011).

DGP surface alloying technology that exhibits high efficiency, good layer uniformity and controllability of layer thickness during the processing was developed, in response to the need for high-quality coatings on the surface of titanium alloys.

This surface technology was used successfully to deposit coatings on steel and cast iron components (Xu et al., 2007). In this paper, however, an Nb coating is deposited on the Ti-Al alloy by means of the DGP technology. The tribological behaviour, oxidation resistance and flame retardancy of Nb-coated and uncoated Ti-Al alloys are analysed and discussed.

## 2. Experimental details

### 2. 1. Specimen preparation

The chemical composition of the Ti-Al-based alloy used in this experiment is presented in Table 1. Each specimen was prepared by cutting into circular disks of 30mm diameter and 5mm thickness. Before the experiment, the specimens were mechanically polished, and then cleaned with ethanol and dried using compressed air.

The operating procedure of the DGP surface alloying technique is described in detail in (Xu, Liu, Zhang, Zhang, Zhang, and He, 2007).; here, it is only explained briefly. An Nb target (∅100mm×5mm) with 99.9% purity was prepared via the powder metallurgy method, and it was used as an Nb source electrode for supplying the alloying element during deposition. The sample was placed on a platform inside a double walled, water-cooled vacuum chamber, and the anode and cathode were each connected to DC power supplies. The potential difference between the cathode and the source electrode resulted in an unequal potential, leading to the hollow cathode effect. Once the given voltage was applied, both the cathode and the source electrodes were surrounded by the glow discharge. Nb ions were sputtered from the source electrode and deposited onto the substrate due to the bias gradient. With the

bombardment of the ions, the desired alloying elements were sputtered from the source electrode, accelerated towards the sample and forced to diffuse into the sample's surface. The process parameters were the following: temperature — 900–1000 °C; source electrode voltage — 900V–950V; substrate voltage — 450V–500V; working pressure — 40 Pa; parallel distance between the source electrode and the substrate — 20mm; treatment time — 3 h.

2. 2. Microstructure analysis

The morphology of the cross-sectional microstructure was investigated using a JSM-6360LV scanning electron microscope (SEM), and the alloying elements' distribution was measured by using an energy dispersive spectrometer (EDS). The phases of surface-alloyed layers were determined via Bruker D8-ADVANCE X-ray diffraction (XRD) with Cu $K_{\alpha}$ radiation.

2. 3. Experiments

2. 3. 1. Sliding friction tests

Sliding friction tests were conducted on uncoated and Nb-coated samples using an HT-500 ball-on-disk tribometer in air at room temperature (20°C±4°C), and room relative humidity (45±5 %) under dry sliding conditions. GCr15 balls with a diameter of 3 mm were used as the counterface material. According to our former experiments and related articles(Cong et al., 2010); Qin et al., 2009); Wang et al., 2013)., the tests were conducted at a range of speeds between 448 and 1120rpm for 10 min with a load of 2.25 N. The rotating radius was 3 mm. This test standard was referred to ASTM G99-05 (Standard, 2005).

2. 3. 2. Oxidation tests

Titanium alloys are often required to perform at temperatures over 600 °C. This resulted in extensive research and development in the application of titanium alloys at elevated temperatures (Peters, Hemptenmacher, Kumpfert, and Leyens, 2003). In this paper, oxidation tests were performed in a high temperature furnace at 750 °C for 100 h.

Coated specimens were periodically weighed and visually inspected every 10 hours using a precision electronic balance with an accuracy of $10^{-4}$ g. This test was carried out according to ISO standard 21608-2012 (Schütze et al., 2015). The investigations of the microstructure and phase analysis after oxidation were performed using an SEM, an EDS and XRD techniques.

2. 3. 3. Ablation tests

The ablation behaviour of the specimens was tested using an oxyacetylene flame. The pressure values of the oxygen and acetylene were 0.42 and 0.042 MPa, respectively. The inner diameter of the oxyacetylene gun tip was 2.5 mm and the distance between the gun tip and the specimen was 10 mm. During the test, the highest temperature of the oxyacetylene flame reaching the surface of the samples was estimated to be 2000±80 °C. The specimens, fixed to a temperature resistant holder, were exposed to the flame until they melted, and their melt times were recorded. This test was carried out according to the ASTM E458-1972 standard (Ogasawara et al., 2002).

## 3. Results

### 3. 1. Microstructure and phrase composition

Fig. 1(a) shows the SEM image of the cross-section morphology of Nb-coated Ti-Al, consisting of two layers, i.e., a deposition layer and a diffusion layer. Many banding phases precipitate in the diffusion region. The results of the line scanning of the Nb-coated Ti-Al alloy investigated using an EDS are shown in Fig. 1(b). Fig. 2 illustrates the X-ray diffraction pattern of Nb-coated Ti-Al; the main phases consisted of Nb, AlNb2, AlMoTi2 and β-Ti.

### 3. 2. Friction and wear tests

Fig. 3 shows the friction coefficient evolution of uncoated and Nb-coated Ti-Al alloys as a function of the sliding distance at room temperature. The friction coefficient of the uncoated Ti-Al alloy was larger (0.44–0.48) than that of Nb-coated Ti-Al alloy (0.27).

Fig. 4 shows the surface morphologies of worn, uncoated and Nb-coated Ti-Al alloys. The wear trace of the Nb-coated sample was shallower than that of the uncoated Ti-Al alloy.

### 3. 3. Oxidation tests

Fig. 5 shows the oxidation kinetics curves of uncoated and Nb-coated Ti-Al alloys at 750 °C during the 100 h test. After 100 h exposure at 750 °C, the mass gain for the Nb-coated Ti-Al alloy was 6.62 mg/cm$^2$, which was much lower than that of the uncoated Ti-Al alloy — 13.97 mg/cm$^2$.

Fig. 6 illustrates the XRD pattern of the uncoated and Nb-coated Ti-Al alloys oxidized at 750 °C for 100 h. It can be seen from Fig. 6 (a) that peaks originating

from $TiO_2$ are dominant in oxidized, uncoated Ti-Al alloys in the presence of $Al_2O_3$, while the surface of the Nb-coated Ti-Al alloy consisted of $Nb_2O_5$ and $TiO_2$ (Fig. 6 (b)).

The SEM surface morphologies of uncoated and Nb-coated Ti-Al alloys after oxidation at 750 °C for 100 h are presented in Fig. 7. Fig. 7 (a) shows the surface of an uncoated Ti-Al alloy covered with an oxide layer with cracks. Fig. 7 (b) shows porous oxides appearing at the interface, which can help oxygen to penetrate the surface (Wen-bo et al., 2007). The oxide layer of the Nb-coated Ti-Al alloy, shown in Figs. 7 (c) and 7 (d), was microstructurally compact and smooth.

3. 4. Ablation tests

The ablation test results show that the average melting time of the uncoated Ti-Al alloy was 136s, and 220s for the Nb-coated Ti-Al alloy. The ablation test proved that the Nb-coated Ti-Al alloy exhibits good flame retardancy.

Fig. 8 shows the surface morphologies of uncoated and Nb-coated Ti-Al alloys after ablation. In Figs. 8 (a) and (b), the cracking and spalling of the uncoated Ti-Al alloy can be seen. The Nb-coated surface (Figs. 8 (c) and (d)) indicated that the oxides exhibited excellent tenacity, which can prevent the diffusion of oxygen into the substrate (Zhao et al., 1999).

## 4. Discussion

It has been shown that Nb was deposited successfully on the Ti-Al alloy by means of the DGP technique. The morphology of the Nb-coated Ti-Al alloy revealed a uniform and compact layer (Fig. 1). The main phases of the Nb-coated Ti-Al alloy

were identified as Nb, AlNb2, AlMoTi2 and β-Ti, with no α-Ti phase (Fig. 2). The structure of the Nb and β-Ti phase is that of a body-centred cubic lattice, with the atomic radius of 1.47 Å. When the temperature reaches 850 °C, Nb and β-Ti phases can mix with each other at any proportion. In addition, when the content of Nb is raised to as high as 50 %, the structure becomes a solid solution of the β-Ti phase (Abdel-Hady et al., 2007); Lee et al., 2000); Zhou et al., 2011).

Friction tests showed that the coefficient of the friction of the Nb-coated Ti-Al alloy was lower and more stable than that of the uncoated Ti-Al alloy (Fig. 3). The initial friction coefficient of the Nb-coated Ti-Al alloy was relatively high because of surface roughness, and it decreased gradually with further increases to the sliding time. It has been suggested that the oxide film that forms on the Nb-coated Ti-Al alloy can act as a lubricant(Miyoshi et al., 2003).

The oxidation test revealed that the mass gain of the Nb-coated Ti-Al alloy was much lower than that of the uncoated alloy (Fig. 5). The Nb-coated Ti-Al alloy was also covered with small and compact oxide grains without visible cracking or spalling after undergoing a 100 h isothermal oxidation test (Fig. 6). The $Nb^{5+}$ phase has a higher valence state than that of $Ti^{4+}$; therefore, substituting $Nb^{5+}$ for titanium ions in $TiO_2$ can decrease the vacancies and diffusion of oxygen effectively. During the oxidation, the oxygen ion migrated from outside to inside, with the niobium ion migrating from inside to outside. The oxygen ion has experienced a process: 1. Adsorbed on the surface of niobium. 2. Inward diffusion 3. Meet the niobium ion. 4. Form the niobium oxide. So the dense $Nb_2O_5$ film covering is not only prevented

oxygen diffusing into the substrate, but also stopped Ti from diffusing outwards(Stroosnijder et al., 1996); Wang et al., 2007).

The flame retardancy of the Nb-coated Ti-Al alloy is caused by the diffusion of Nb into the surface, leading to microstructure distortion. This restrains growth during the β phase and enhances surface stabilization under conditions of thermal exposure. In contrast, the poor resistance of titanium alloy to high temperatures is due to the diffusion of oxygen into the substrate through the micropores and cracks (Zhao, Zhou, and Deng, 1999). The presence of the $Nb_2O_5$ layer on the surface of the Ti-Al alloy prevents both the diffusion of oxygen into the substrate and the outward diffusion of Ti. As a result, the flame retardancy of the Ti-Al alloy is effectively improved.

## 4. Conclusion

A Ti-Nb diffusion layer was obtained on a Ti-Al alloy by means of the DGP technology. The Nb-coated Ti-Al alloy exhibits better wear resistance compared to that of the uncoated Ti-Al alloy. It has been observed that the third-party abrasive wear, caused by wear debris, increases the friction coefficient of the uncoated Ti-Al alloy. The improvement of the high-temperature oxidation resistance of Nb-coated Ti-Al alloy is due to $Nb^{5+}$ ions contributing to the decrease of vacancies in the lattice and the diffusion rate of oxygen into the substrate. The microstructure distortion of the lattice caused by Nb restrains the growth of the β phase and enhances the surface-active stabilization under thermal exposure conditions. It is also concluded that Nb can improve the flame retardancy of the Ti-Al alloy effectively.

## Acknowledgements

This project was supported by National Natural Science Foundation of China (Grant No. 51175247), Natural Science Foundation for Young Scientists of Jiangsu Province, China (Grant No. BK20140819) and the Priority Academic Program Development of Jiangsu Higher Education Institutions.

## References

M. Abdel-Hady, et al. (2007) 'Phase stability change with Zr content in beta-type Ti-Nb alloys', Scripta Materialia, Vol. 57 No. 11, pp. 1000-1003 <Go to ISI>://WOS:000250242100007 (Access 2007).

W. Cong, et al. (2010) 'Sliding wear of low carbon steel modified by double-glow plasma surface alloying with nickel and chromium at various temperatures', Wear, Vol. 268 No. 5-6, pp. 790-796 <Go to ISI>://WOS:000275158000021 (Access 2010).

F. El-Hossary, et al. (2015) 'Tribo-mechanical and electrochemical properties of plasma nitriding titanium', Surface and Coatings Technology, Vol. 276, pp. 658-667 (Access 2015).

R. Godley, et al. (2006) 'Corrosion behavior of a low modulus beta-Ti-45%Nb alloy for use in medical implants', Journal of Materials Science-Materials in Medicine, Vol. 17 No. 1, pp. 63-67 <Go to ISI>://WOS:000234396400008 (Access 2006).

J.Y. Lee, et al. (2000) 'Effect of Mo and Nb on the phase equilibrium of the Ti-Cr-V ternary system in the non-burning beta-Ti alloy region', Journal of Alloys and Compounds, Vol. 297 No. 1-2, pp. 231-239 <Go to ISI>://WOS:000084513000039 (Access 2000).

C. Leyens and M. Peters (2003) Titanium and titanium alloys, Wiley Online Library. Access 2003).

K. Miyoshi, et al. (2003) 'Fretting wear of Ti-48Al-2Cr-2Nb', Tribology International, Vol. 36 No. 2, pp. 145-153 <Go to ISI>://WOS:000180233800009 (Access 2003).

D. Nolan, et al. (2006) 'Sliding wear of titanium nitride thin films deposited on Ti–6Al–4V alloy by PVD and plasma nitriding processes', Surface and Coatings Technology, Vol. 200 No. 20, pp. 5698-5705 (Access 2006).

T. Ogasawara, et al. (2002) 'Thermal response and ablation characteristics of carbon fiber reinforced composite with novel silicon containing polymer MSP', Journal of composite materials, Vol. 36 No. 2, pp. 143-157 (Access 2002).

M. Peters, et al. (2003) 'Structure and properties of titanium and titanium alloys', Titanium and Titanium Alloys: Fundamentals and Applications, pp. 1-36 (Access 2003).

L. Qin, et al. (2009) 'Study on Microstructure and Wear Resistance of Cr-Mo Surface Modified Layer on Ti6Al4V by Double-Glow Plasma Technique', Rare Metal

Materials and Engineering, Vol. 38 No. 12, pp. 2226-2229 <Go to ISI>://WOS:000273671400035 (Access 2009).

T.R. Rautray, et al. (2011) 'Ion implantation of titanium based biomaterials', Progress in Materials Science, Vol. 56 No. 8, pp. 1137-1177 (Access 2011).

M. Schütze, et al. (2015) 'Oxidation‐related life‐time assessment using the new ISO standards ISO 21608: 2012 and ISO 26146: 2012', Materials and Corrosion, (Access 2015).

A. Standard (2005) 'G99-05,‘‘', Standard Test Method for Wear Testing with a Pin-on-Disk Apparatus’’, ASTM International, West Conshohocken, PA, (Access 2005).

M. Stroosnijder, et al. (1996) 'The effect of niobium ion implantation on the oxidation behavior of aγ-TiAl-based intermetallic', Oxidation of Metals, Vol. 46 No. 1-2, pp. 19-35 (Access 1996).

L. Wagner and M. Wollmann (2013) 'Titanium and Titanium Alloys', Structural Materials and Processes in Transportation, pp. 151-180 (Access 2013).

M. Wang, et al. (2004) 'Study on creep behavior of Ti–V–Cr burn resistant alloys', Materials Letters, Vol. 58 No. 26, pp. 3248-3252 (Access 2004).

Q. Wang, et al. (2013) 'Microstructure and sliding wear behavior of pure titanium surface modified by double-glow plasma surface alloying with Nb', Materials & Design, Vol. 52, pp. 265-273 <Go to ISI>://WOS:000323832200029 (Access 2013).

W.B. Wang, et al. (2007) 'Plasma niobium surface alloying of pure titanium and its oxidation at 900 degrees C', Chinese Journal of Aeronautics, Vol. 20 No. 2, pp. 111-114 <Go to ISI>://WOS:000255391000003

W. Wen-bo, et al. (2007) 'Plasma niobium surface alloying of pure titanium and its oxidation at 900 degrees C', Chinese Journal of Aeronautics, Vol. 20 No. 2, pp. 111-114 (Access 2007).

Z. Xu, et al. (2007) 'Double glow plasma surface alloying and plasma nitriding', Surface & Coatings Technology, Vol. 201 No. 9-11, pp. 4822-4825 <Go to ISI>://WOS:000246509400005 (Access 2007).

Y. Zhao, et al. (2000) 'Microstructures of a burn resistant highly stabilized β-titanium alloy', Materials Science and Engineering: A, Vol. 282 No. 1, pp. 153-157 (Access 2000).

Y.Q. Zhao, et al. (1999) 'The role of interface in the burning of titanium alloys', Materials Science and Engineering a-Structural Materials Properties Microstructure and Processing, Vol. 267 No. 1, pp. 167-170 <Go to ISI>://WOS:000081293000019 (Access 1999).

Z.C. Zhou, et al. (2011) 'Anelastic relaxation caused by interstitial atoms in beta-type sintered Ti-Nb alloys', Journal of Alloys and Compounds, Vol. 509 No. 27, pp. 7356-7360 <Go to ISI>://WOS:000291248400009 (Access 2011).

Table 1 Chemical composition of the Ti-Al alloy (wt %).

| Ti | Al | Mo | Zr | Si | O | C | N |
|---|---|---|---|---|---|---|---|
| Base | 6.5 | 3.3 | 1.5 | 0.25 | ≤0.015 | ≤0.1 | ≤0.05 |

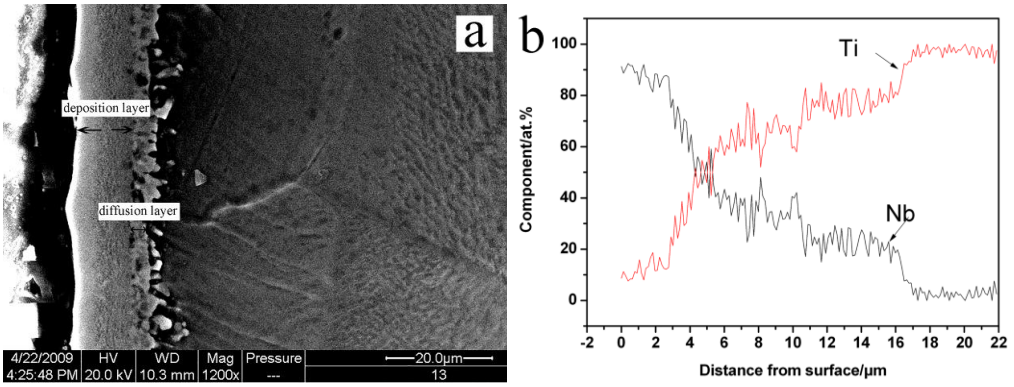


Fig. 1 (a) Cross-section SEM morphology of Nb-coated Ti-Al, (b) Line scanning results of Nb-coated Ti-Al.

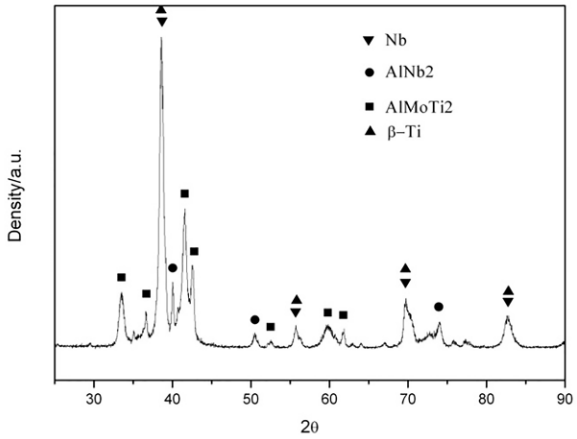


Fig. 2 X-ray diffraction pattern of Nb-coated Ti-Al.

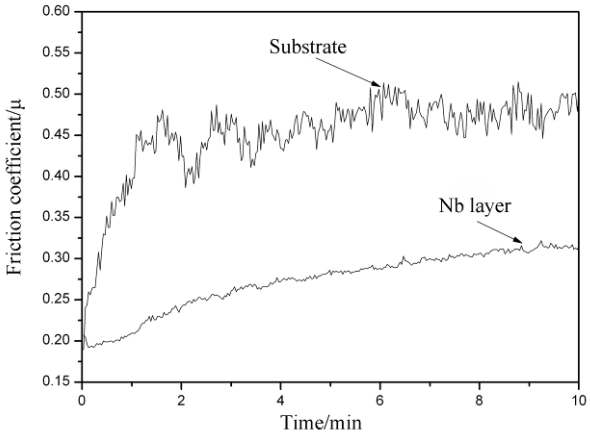


Fig. 3 Friction coefficients of uncoated and Nb-coated Ti-Al alloys at room temperature.

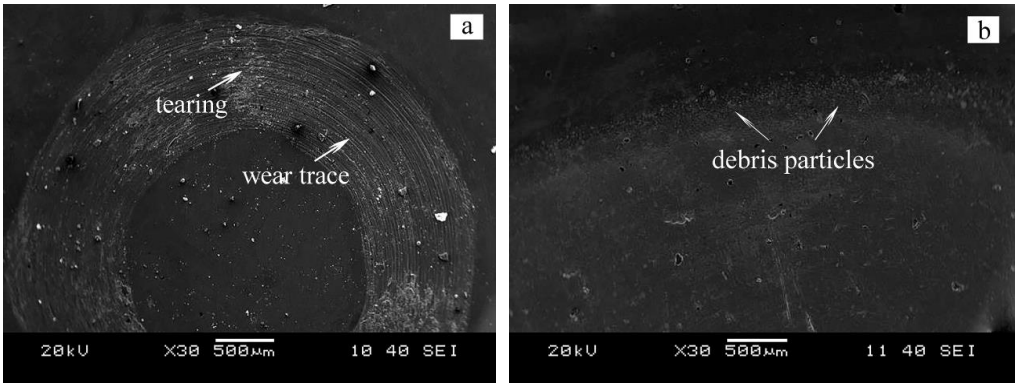


Fig. 4 Surface morphologies of worn (a) uncoated and (b) Nb-coated Ti-Al alloys.

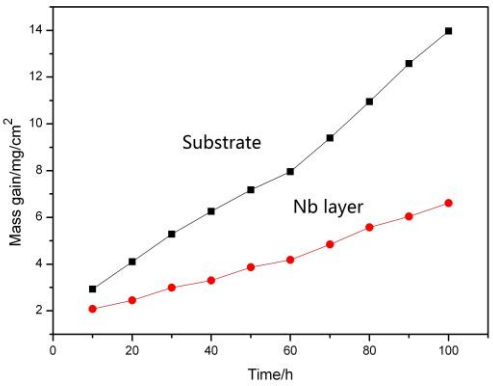


Fig. 5 Oxidation kinetics curves of uncoated and Nb-coated Ti-Al alloys at 750 °C for 100 h.

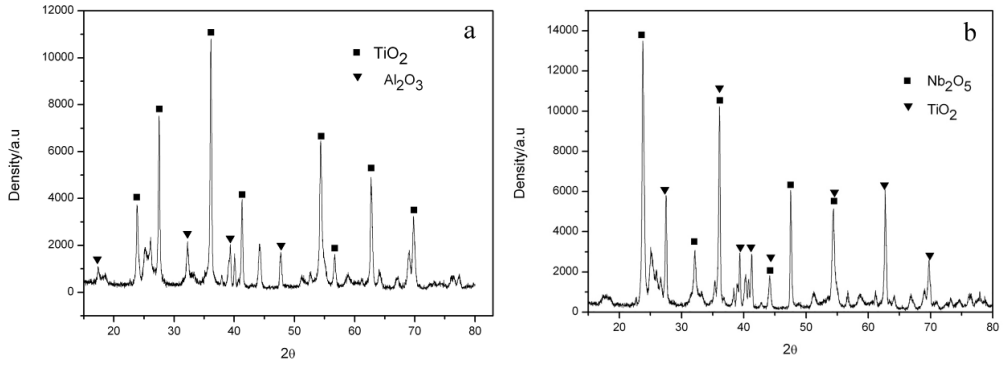


Fig. 6 XRD patterns of (a) uncoated and (b) Nb-coated Ti-Al alloys oxidized at 750 °C for 100 h.

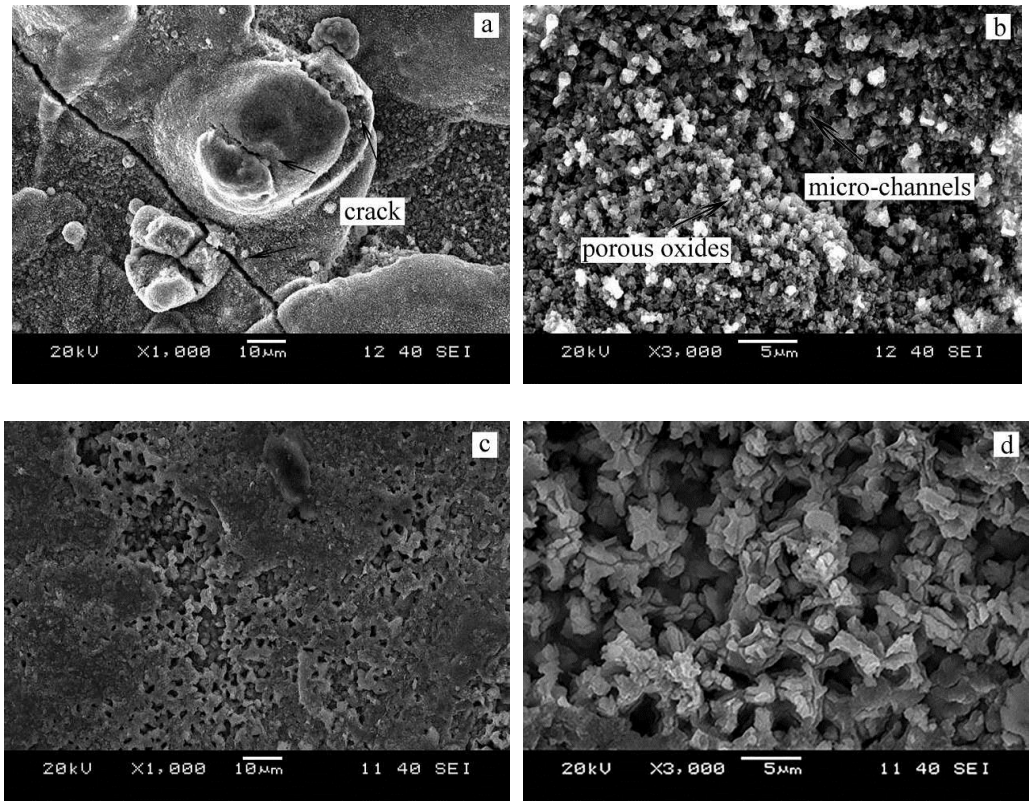


Fig. 7 Surface morphologies of uncoated (a, b), and Nb-coated (c, d) Ti-Al alloys oxidized at 750 °C for 100 h.

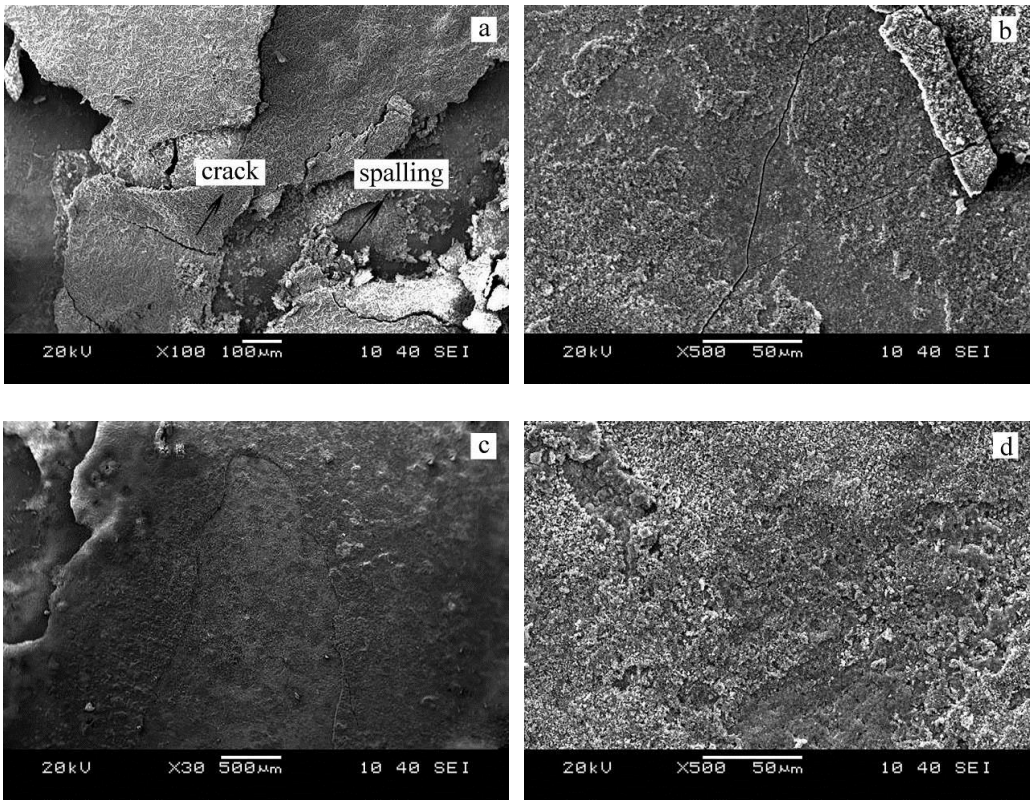


Fig. 8 Ablative central region morphologies of uncoated (a, b), and Nb-coated (c, d) Ti-Al alloys after ablation.